EFFECTS OF CALCIUM ADMINISTRATION ON PARATHYROID GLAND, NaPi 2a COTRANSPORTER AND PTH1R IN AN ANIMAL MODEL OF THE ANDROPAUSE

EFEKTI TRETMANA KALCIJUMOM NA PARATIREOIDNU ŽLEZDU, NaPi 2a KOTRANSPORTER I PTH1R U ANIMALNOM MODELU ANDROPAUZE

Jasmina Živanović[1], Branko Filipović[1], Ivana Medigović[1], Vladimir Ajdžanović[1],
Nikola Tanić[2], Marko Miler[1], Verica Milošević[1]

[1]Department of Cytology, Institute for Biological Research »Siniša Stanković«,
University of Belgrade, Belgrade, Serbia
[2]Department of Neurobiology, Institute for Biological Research »Siniša Stanković«,
University of Belgrade, Belgrade, Serbia

Summary

Background: Increased risk of osteoporotic bone fractures represents the adverse event in andropausal men. Due to diminished calcium absorption in elderly, its supplementation is used for prevention and treatment of advanced-age osteoporosis.
Methods: Sixteen-month-old Wistar rats were divided into sham-operated (SO), orchidectomized (Orx) and Ca^{2+}-treated orchidectomized (Orx+Ca) groups. Ca^{2+} (28.55 mg/kg b.w.) was administered intramuscularly for 3 weeks, while the SO and Orx received vehicle alone. Parathyroid glands (PTG) were analyzed histomorphometrically, while the expression of NaPi 2a mRNA from kidneys was determined by real time PCR. NaPi 2a and PTH1R abundance was detected immunofluorescently. Serum and urine parameters were determined biochemically.
Results: The PTG volume was 15% (p<0.05) greater in Orx rats than in the SO group. In Orx+Ca^{2+} animals, PTG volume was decreased by 17% (p<0.05), when compared to the Orx rats. Orchidectomy led to an increment of serum PTH of 13% (p<0.05) compared to the SO group, while Orx+Ca decreased it by 10% (p<0.05) when compared to Orx animals. The intensity of the NaPi 2a signal was reduced in Orx rats, in comparison with the SO group. Orx+Ca^{2+} treatment increased the abundance of NaPi 2a,

Kratak sadržaj

Uvod: Povećan rizik od preloma kostiju, izazvan osteoporozom, uobičajen je u andropauzi. Usled smanjene apsorpcije kalcijuma kod starijih osoba, on se često koristi u prevenciji i tretmanu osteoporoze u poznom dobu.
Metode: Wistar pacovi stari 16 meseci podeljeni su na lažno operisanu (SO), orhidektomisanu (Orx) i Ca^{2+} tretiranu orhidektomisanu (Orx+Ca) grupu. Ca^{2+} je aplikovan intramuskularno u dozi od 28,55 mg/kg telesne mase, dok su kontrolne grupe SO i Orx primile odgovarajući volumen rastvarača. Paratireoidne žlezde (PTŽ) analizirane su histomorfometrijski, dok je nivo ekspresije gena za NaPi 2a određen pomoću PCR metode u realnom vremenu. Prisustvo NaPi 2a i PTH1R identifikovano je imunofluorescentnom metodom. Parametri iz seruma i urina određeni su biohemijskim metodama.
Rezultati: Volumen PTŽ je povećan za 15% (p<0,05) kod Orx pacova u odnosu na SO grupu. Kod Orx+Ca tretiranih životinja, volumen PTŽ je smanjen za 17% (p<0,05) u poređenju sa Orx pacovima. Orhidektomija je povećala nivo PTH u serumu za 13% (p<0,05) u odnosu na SO grupu, dok je nivo ovog hormona kod Orx+Ca pacova smanjen za 10% (p<0,05) u poređenju sa Orx životinjama. Intenzitet NaPi 2a signala je redukovan kod Orx životinja u odnosu na SO grupu, dok Orx+Ca tretman povećava pri-

Address for correspondence:

Jasmina Živanović, M. Sc., Research Assistant
Institute for Biological Research »Siniša Stanković«
Despot Stefan Blvd. 142, 11060 Belgrade, Serbia
Tel.: +381-11-2078-302; Fax:+318-11-2761-433
e-mail: jasminap@ibiss.bg.ac.rs

compared to the Orx group. In Orx rats, the staining for PTH1R was stronger when compared to the SO group, while the Orx+Ca^{2+} treatment induced reduction of the PTH1R immunofluorescence, compared to Orx animals. Orchidectomy increased Pi urinary concentrations by 8% ($p<0.05$), in comparison with the SO control, while in the Orx+Ca^{2+} group urinary Pi concentration was 5% lower ($p<0.05$) than for the Orx rats.

Conclusions: Our results indicate that Ca^{2+} administration reduces the PTH serum level and the presence of PTH1R, while increased abundance of NaPi 2a cotransporter positively regulates Pi urine reabsorption in an animal model of the andropause.

Keywords: andropause, calcium, NaPi 2a, orchidectomized rats, parathyroid gland, PTH1R

sustvo NaPi 2a, u poređenju sa Orx grupom. Kod Orx pacova, obojenost PTH1R je jača u odnosu na SO grupu, dok je Orx+Ca tretman redukovao imunofluorescencu u poređenju sa Orx životinjama. Orhidektomija je povećala koncentraciju Pi u urinu za 8% ($p<0.05$) u poređenju sa SO kontrolom, dok je Orx+Ca tretman smanjio koncentraciju Pi u urinu za 5% ($p<0.05$) u odnosu na koncentraciju kod Orx pacova.

Zaključak: Prikazani rezultati ukazuju na to da tretman Ca^{2+} smanjuje nivo PTH u serumu kao i prisustvo PTH1R, dok je zastupljenost NaPi 2a kotransportera povećana, što pozitivno reguliše reapsorpciju Pi iz urina u animalnom modelu andropauze.

Ključne reči: andropauza, kalcijum, NaPi 2a, kastrirani pacovi, paratireoidna žlezda, PTH1R

Introduction

Andropause, an age-related syndrome, is in the first instance characterized by lowered circulating testosterone, while the luteinizing hormone (LH) and prolactin levels appear to be normal (1, 2). Also, dehydroepiandrosterone (DHEA), growth hormone (GH), thyroxine (T4) and melatonin blood levels are lowered in andropause, and an increased incidence of cardiovascular issues, benign and malignant prostate diseases, as well as osteoporosis are following these multihormonal alterations (2, 3). It is generally known that steroid hormones represent important regulators of bone resorption and formation (4–6), but their application in the treatment of age-related osteoporosis increases the risk of cardiovascular diseases and prostate cancer (7). Besides steroid hormones, calcium (Ca^{2+}) plays a significant role in bone metabolism in all age groups. Owing to low dietary Ca^{2+} intake in elderly (8), accompanied with low bone mass and increased risk of bone fractures (9), Ca^{2+} administered alone or in combination with vitamin D supplementation is widely used to prevent and treat osteoporosis (10). However, it has been observed that Ca^{2+} supplements are associated with some cardiovascular adverse events, especially with myocardial infarction (11).

The major role in bone metabolism and mineral homeostasis is attributed to parathyroid hormone (PTH), the product of parathyroid glands (PTG). The main regulators of synthesis and secretion of PTH are low serum Ca^{2+} concentration, mediated through calcium-sensing receptor (CaR) (12), and high serum phosphorus (Pi). Halloran et al. (13) established that PTG volume and serum PTH level increase in both rats and humans during ageing. Increased PTH level contributes to bone loss and also induces phosphaturia (14, 15), by binding to parathyroid hormone receptor type 1 (PTH1R) in bone tissue and epithelial cells of the kidney proximal tubules. Sodium-phosphate cotransporter type 2a (NaPi 2a) represents one of the main regulators of Pi reabsorption from primary urine in the kidney proximal tubules. Abundance and activity of NaPi 2a is regulated with a variety of stimuli, including dietary phosphate intake, PTH, glucocorticoids and steroid hormones (15).

The positive impact of steroid hormones on the maintenance of calcium balance reflects on the gastrointestinal absorption and renal tubular reabsorption of calcium (16). Our previous studies have shown that the orchidectomy-induced lack of steroid hormones caused an enhancement in urinary Ca^{2+} excretion and decreased serum Ca^{2+} and Pi concentrations (17, 18), along with an increment in Pi urinary wasting, in middle-aged male rats (19). These changes have led to a decrease in the bone tissue compactness (17, 18), which increases the risk of bone fragility (9).

Due to the scarce evidence on the influence of Ca^{2+} treatment on regulation of Pi homeostasis, the aim of this study was to examine the effects of Ca^{2+} application on PTG, functionally related NaPi 2a cotransporter and PTHR, in kidney tubules of orchidectomized male rats, as an animal model of the andropause.

Materials and Methods

Experimental design

Middle-aged (16-month-old) Wistar male rats, bred at the Institute for Biological Research, Belgrade, Serbia, were maintained under standard laboratory conditions ($22\pm2°C$, 12–12 h light–dark cycle). Food and water were available *ad libitum*.

At the age of 15 months, animals (n=24) were divided into three groups. The first group of animals (n=8) was sham-operated (SO), while the other group (n=16) was bilaterally orchidectomized (Orx), under ketamine anesthesia (ketamine hydrochloride; Richter Pharma, Wels, Austria; 15 mg/kg b.w.). After 2 weeks of recovery, Orx animals were divided into two groups of eight animals each. One group of Orx rats was intramuscularly (i.m.) given Ca-glubionate (Novartis, Switzerland) (Orx+Ca^{2+}; 28.55 mg/kg b.w.) every

day, for 3 weeks. The other Orx group and the SO group were treated with the vehicle, following the same regime, and they served as controls. Before sacrifice, urine samples were collected for Ca^{2+} and Pi analyses. The rats were decapitated 24 h after the last injection. Blood samples were collected from the trunk and stored at -80 °C until analysis. All animal procedures were in compliance with the EEC Directive (86/609/EEC) on the protection of animals used for experimental and other scientific purposes, and were approved by the Ethical Committee for the Use of Laboratory Animals of the Institute for Biological Research »Siniša Stanković«, University of Belgrade.

Histological and electron microscopy analysis

Thyroid-parathyroid tissue for the histological analysis was excised from six animals per group, fixed in Bouin's solution for 48 h, embedded in paraplast and serially cut, using a rotational microtome (Leica, Germany), at 3 μm thickness. The sections were stained with hematoxylin/eosin and mounted with DPX (Sigma-Aldrich, Co., USA).

For the electron microscopy analysis, thyroid-parathyroid glands were removed from the remaining two animals per group, and immediately after decapitation cut into slices. Tissue slices were immersed in 4% glutaraldehyde solution in 0.1 mol/L phosphate buffer (PB) (pH 7.4) for 24 h, and postfixed with 1% OsO_4 in the same buffer for 1 h. The samples were embedded in Araldite and Harderner resin and cut in ultrathin sections on an LKB ultramicrotome III (type 8802A; Sweden), with a Diatome ultra 45° diamond knife (Diatome, Switzerland). Grids with thin sections were stained with uranylacetate and leadcitrate, and examined under a MORGAGNI 268 (FEI Company, USA) transmission electron microscope.

Stereological measurements

The volume of PTG was estimated using Cavalieri's principle (20) with a newCAST stereological software package (VIS–Visiopharm Integrator System, version 2.12.1.0; Visiopharm; Denmark). Every 30th section from each of the tissue blocks was analyzed. The PTG volume (Vptg) was calculated by the formula:

$$\overline{V}_{ptg} = a(p) \cdot \overline{d} \cdot \sum_{i=1}^{n} Pi$$

where $a(p)$ is the area associated with each sampling point (10956.52 μm^2); $\overline{d}$ is the mean distance between two consecutively studied sections (90 μm); n is the number of sections studied for each PTG; and ΣPi is the sum of points hitting a given target. The volume density of chief cells (V_{vcc}) and interstitium (blood vessels and connective tissue, Vvi) were determined for every sampled section.

Immunofluorescent studies

The kidneys were fixed in formalin solution at room temperature for 48 h, embedded in paraplast, and sectioned at 3 μm. For the immunofluorescence staining, sections were deparafinised and dehydrated, while antigen retrieval was performed in 0.1 mol/L citrate buffer solution (pH 6.0). Sections were washed in PBS and pretreated with blocking normal donkey serum (Dako, Denmark), diluted in PBS (1:10). After blocking, they were incubated overnight at room temperature, with rabbit anti-rat NaPi 2a antibody (1:100; kindly donated by Dr Jürg Biber, Institute of Physiology, University of Zurich, Zurich, Switzerland) or PTH1R antibody (1:100, Abcam, Cambridge, UK). After rinsing in PBS, the sections were covered for 2 h at room temperature with secondary antibody Alexa Fluor 555 donkey anti-rabbit IgG (1:200; Molecular Probes, Inc., USA). Finally, they were rinsed five times in PBS. Sections were cover slipped using Mowiol 4–88 (Sigma-Aldrich, Co., USA) and examined with a Carl Zeiss AxioVision microscope (Zeiss, Germany).

RT-PCR

Total RNA was isolated from the rat kidney cortex using TRIzol Reagent (Life Technologies, USA) according to the manufacturer's instructions. RNA was quantified by spectrophotometry, and cDNA was synthesized using a cDNA Reverse Transcription kit (Applied Biosystems, USA). PCR amplification of cDNA was performed in ABI Prism 7000 (Applied Biosystems) using SYBRGreen (Applied Biosystems) as follows: 2 minutes at 50 °C for dUTP activation, 10 minutes at 95 °C for initial denaturation of cDNA, followed by 40 cycles, each consisting of 15 s of denaturation at 95 °C and 60 s at 60 °C for primer annealing and chain extension. Primer pairs were the following: NaPi 2a, forward, 5'-GCCACTTCTTCTT CAACATC-3'; reverse, 5'-CACACGAGGAGGTA-GAGG-3'; cyclo A forward 5'-CAAAGTTCCAAA-GACAGCAGAAAA-3'; reverse, 5'- CCACCCTGGCA-CATGAAT-3'. The expression level of each gene was calculated using the formula $2^{-(Cti-Cta)}$, where Cti is the cycle threshold value of the gene of interest and Cta was the cycle threshold value of cyclophilin A as a reference gene. All of the data were calculated from triplicate reactions. RNA data are presented as average relative levels vs. cyclophilin A±SD.

Biochemical analyses

Serum PTH concentration was measured in duplicate samples without dilution, using a Rat Intact PTH ELISA Kit (Immunotopics, Inc., San Clemente, CA, USA), within a single assay. The intra-assay coef-

ficient of variation (CV) was 2.4%. The lowest concentration of rat intact PTH measurable by this kit is 1.6 pg/mL (the assay sensitivity). Serum concentrations of Ca^{2+} and Pi, and urinary concentration of Pi were determined on a Hitachi 912 analyzer (Roche Diagnostics GmbH, Mannheim, Germany).

Statistical analysis

STATISTICA® version 6.0 (StatSoft, Inc) was used for the statistical analysis. All results were expressed as mean ± SD. Differences between the groups were assessed by one-way analyses of variance (ANOVA) followed by Duncan's multiple range tests for post hoc comparisons between groups. Values of $p < 0.05$ were considered statistically significant.

Results

Histological findings in the parathyroid glands

The parathyroid glands (PTG) in all groups were localized laterally in the thyroid gland lobes. They typ-

ically possessed an oval shape and were surrounded with a connective tissue capsule. The chief cells were densely packed in cords or clusters around and along capillaries, with spherical to oval or elongated nuclei. PTG in SO rats had an apparent connective tissue capsule, while the chief cells (white arrows) were separated with a delicate stroma of connective tissue and blood vessels (Figure 1A, black arrows). PTG in the Orx group were larger, with numerous chief cells (white arrows) and noticeable interstitium, in comparison with SO (Figure 1B, black arrows). After Ca^{2+} treatment (Orx+Ca), PTGs were smaller, with a more massive interstitium compared to the glands in Orx animals (Figure 1C, black arrows).

Ultrastructural observations in the parathyroid glands

Ultrastructural analyses of PTG in the SO group demonstrated compactly arranged chief cells, with numerous folds and interdigitations of the cell membrane. Rough endoplasmatic reticulum (RER, white arrows) and the Golgi complex (black arrows) were
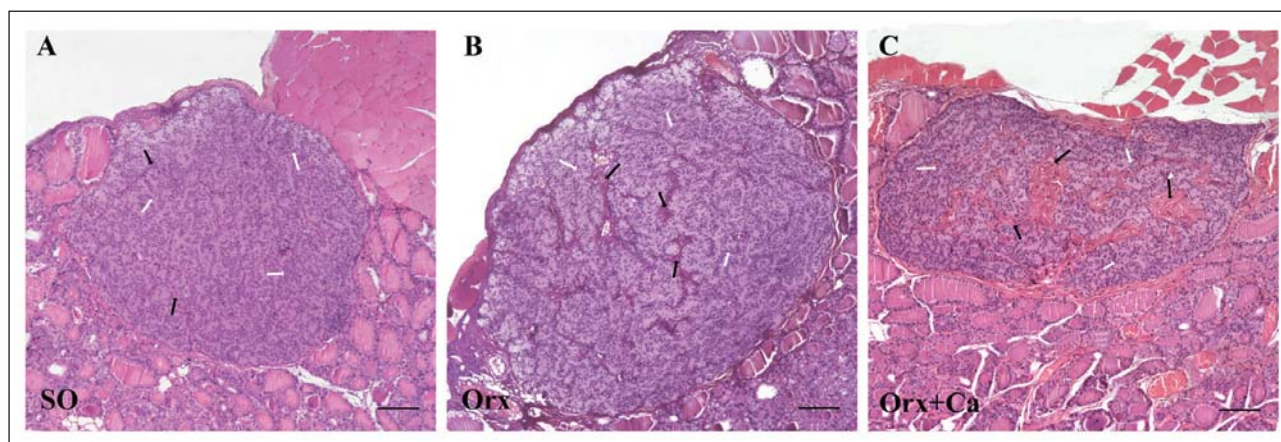

Figure 1 Sections of PTG from A) sham-operated (SO), B) orchidectomized (Orx) and C) orchidectomized rats treated with Ca^{2+} (Orx+Ca). Chief cells (white arrows) and interstitium (black arrows) are clearly visible. Hematoxylin-eosin staining, scale bar – 100 μm.
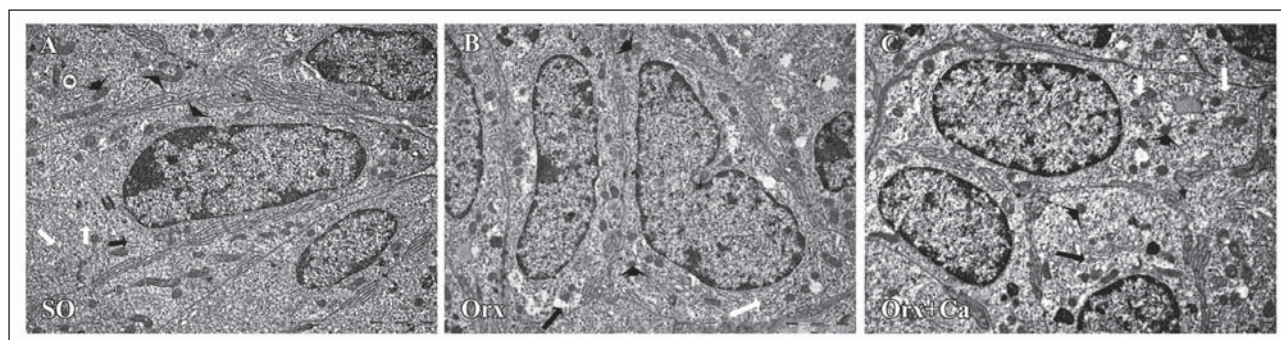

Figure 2 Ultrathin sections of PTG chief cells from A) sham-operated (SO), B) orchidectomized (Orx) and C) orchidectomized rats treated with Ca^{2+} (Orx+Ca). RER (white arrows), Golgi complex (black arrows) and mitochondria (black arrow head) are marked as the representative structures. Scale bar – 500 nm.
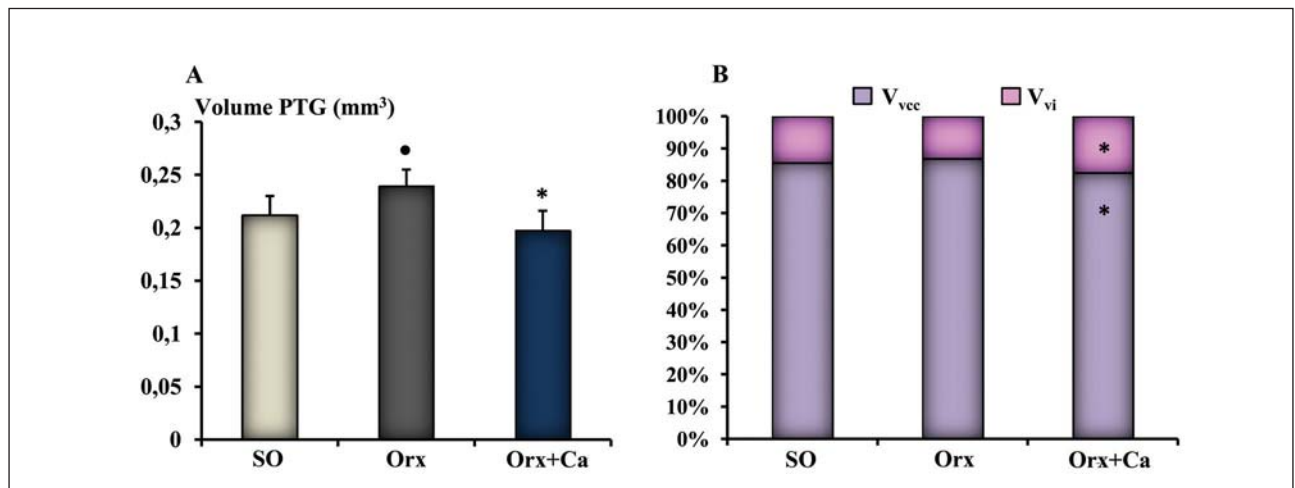
Figure 3 A) The volume of PTG in sham-operated (SO), orchidectomized (Orx) and orchidectomized rats treated with Ca^{2+} (Orx+Ca). All values are presented as mean±SD; ap<0.05 vs. SO, bp<0.05 vs. Orx. B) Volume density of chief cells (Vvcc) and interstitium (Vvi) in sham-operated (SO), orchidectomized (Orx) and orchidectomized rats treated with Ca^{2+} (Orx+Ca). All values are presented as mean±SD; •p<0.05 vs. SO, *p<0.05 vs. Orx.
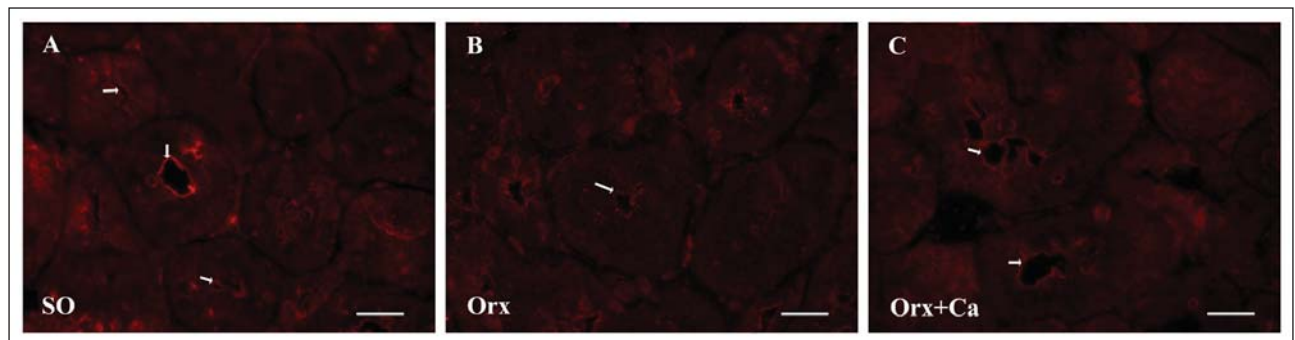

Figure 4 Localization of NaPi 2a cotransporter in epithelial cells of proximal tubules. A) In the sham-operated (SO) group of animals NaPi 2a was strongly labeled in the apical brush border pole of proximal tubule epithelial cells; B) NaPi 2a staining intensity in the apical domain of proximal tubule cells was decreased after orchidectomy (Orx). C) After Ca^{2+} treatment (Orx+Ca) the intensity of NaPi 2a labeling was slightly increased. Paraffin sections, immunofluorescence, scale bar – 10 μm.

moderately developed while mitochondria (black arrow heads) were dispersed throughout the cytoplasm. Nuclei were elongated and located near the apical domain of the cells (*Figure 2A*). Interdigitations of the plasma membrane in Orx animals were more numerous than in the chief cells of SO animals. The RER (white arrows) and Golgi complex (black arrows) were more developed than in the SO group, with abundant mitochondria (black arrow heads) and larger centrally located nuclei (*Figure 2B*). Ultrastructural micrographs of chief cells from Orx animals treated with Ca^{2+} (Orx+Ca) showed less prominent plasma membrane interdigitations. The RER (white arrows) and Golgi complex (black arrows) were poorly represented with fewer and smaller mitochondria (black arrow heads), in comparison with the Orx animals (*Figure 2C*).

PTG volume

In SO middle-aged male rats PTG volume was 0.21±0.02 mm³. In Orx rats, PTG volume was 15% (p<0.05) greater than in the SO group (*Figure 3A*). After Ca^{2+} treatment (Orx+Ca), PTG volume was decreased by 17% (p<0.05), when compared to the values of the Orx animals (*Figure 3A*). In the Orx group of animals, volume density (Vvcc) of the PTG chief cells was slightly raised by 2% (p<0.05) in comparison with the SO group, while the treatment with Ca^{2+} (Orx+Ca) induced a 4% decrease of Vvcc (p<0.05), when compared to Orx animals (*Figure 3B*). After Ca^{2+} treatment (Orx+Ca), the volume density of interstitium (Vvi) in PTG was increased by 25% (p<0.05), in comparison with the Orx group of animals (*Figure 3B*).

Immunofluorescent appearance of NaPi 2a and PTH1R

Kidney sections of all experimental groups were immunofluorescently stained with the specific anti-body for NaPi 2a and PTH1R. Kidney sections of SO rats showed a strong NaPi 2a signal in the microvilli of the border brush membrane (BBM, white arrows), in proximal tubule cells (*Figure 4A*). In Orx group, the intensity of the NaPi 2a signal in BBM was reduced, in comparison with SO animals (*Figure 4B*, white arrow). Treatment with Ca^{2+} (Orx+Ca^{2+}) slightly increased the abundance of NaPi 2a in the brush bor-der of the proximal tubules (white arrows), in compar-ison with the Orx group of animals (*Figure 4C*). The immunofluorescent labeling of PTH1R, in the proxi-mal tubules of SO animals, showed basolateral local-ization of PTH1R in the epithelial cells of the proximal kidney tubules (*Figure 5A*). In Orx animals, the stain-ing for PTH1R was stronger when compared to SO animals (*Figure 5B*), while the treatment with Ca^{2+} (Orx+Ca^{2+}) induced some reduction of the immuno-fluorescent signal in the basolateral domain of proxi-mal tubule epithelial cells (*Figure 5C*).

RT-PCR

Analysis of the NaPi 2a mRNA level revealed that Orx decreased NaPi 2a mRNA compared to the SO group of animals, while Ca^{2+} administration led to a slight increase in the NaPi 2a mRNA expression level, in comparison with Orx animals (*Figure 6*).

Biochemical findings

Biochemical findings are shown in *Table I*. Orchidectomy induced a 13% increase in serum PTH (p<0.05), when compared to SO animals. After treatment with Ca^{2+} (Orx+Ca), serum PTH concen-tration was 10% lower (p<0.05) than in the Orx group. In the Orx group, the concentrations of Ca^{2+} and Pi were decreased by 3% and 4% (p<0.05) respectively, in comparison with the SO group. In Orx+Ca animals, serum concentrations of Ca^{2+} and Pi were 3% and 10% (p<0.05) higher, respectively, than in Orx animals. Orchidectomy increased Pi uri-nary concentrations by 8% (p<0.05), in comparison with the SO control, while urinary Pi concentration
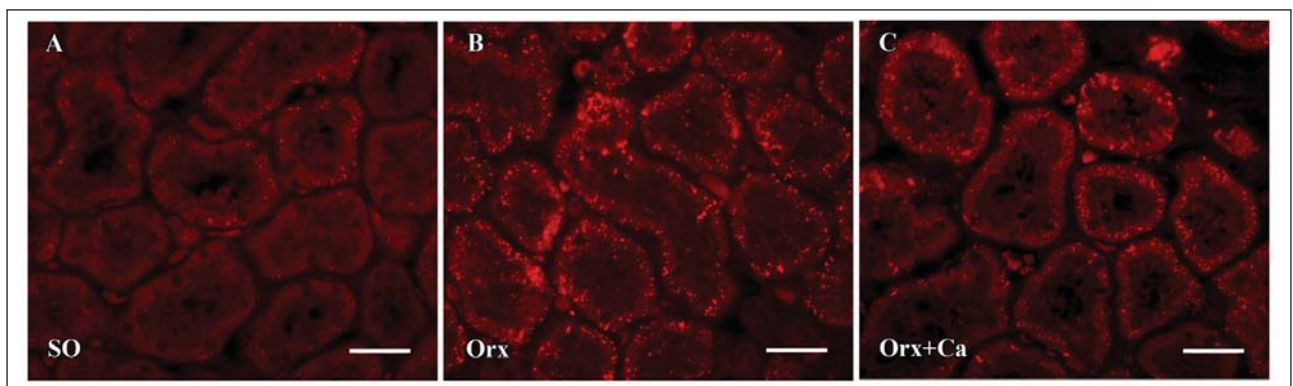

Figure 5 Immunofluorescence imaging of PTH1R in epithelial cells of proximal tubules. A) Kidney section of SO animals showed prevalent basolateral in relation to apical localization of PTH1R often seen in a punctuate pattern. B) Considerably stronger PTH1R staining was present in orchidectomized rats (Orx). C) After Ca^{2+} treatment (Orx+Ca) weaker abundance of PTH1R was present. Paraffin sections, immunofluorescence, scale bar – 10 μm.
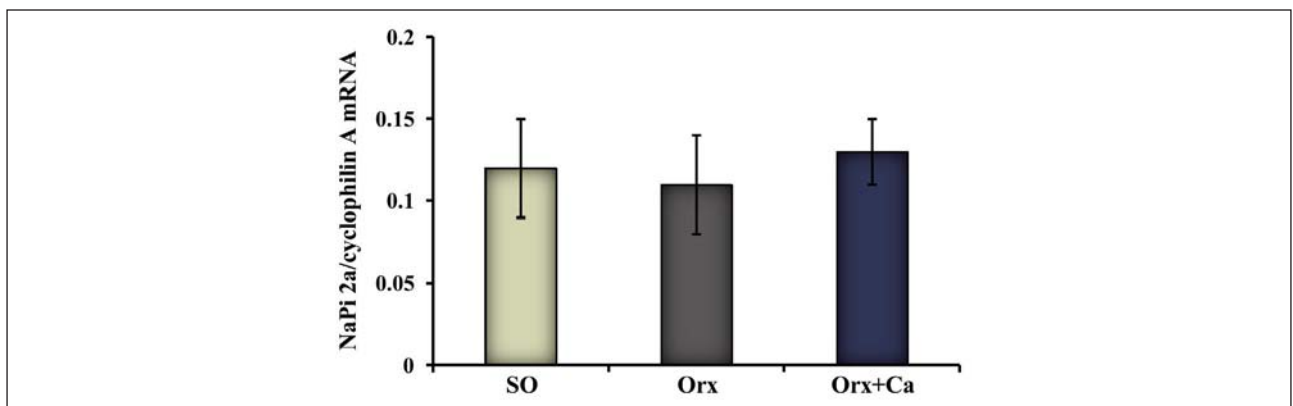

Figure 6 Real-time PCR analyses for NaPi 2a mRNA in control (SO), orchidectomised (Orx) and orchidectomized rats treated with Ca^{2+} (Orx+Ca); data are presented as relative expression of mRNA.

Table I Serum and urine parameters in sham-operated (SO), orchidectomized (Orx) and orchidectomized rats treated with Ca^{2+} (Orx+Ca) group.

	SO	Orx	Orx+Ca
PTH (ng/L)	65.96±3.96	74.57±2.24 •	67.7±5.13 *
Serum Ca^{2+} (mmol/L)	2.32±0.03	2.26±0.06 •	2.33±0.03 *
Serum Pi (mmol/L)	1.93±0.05	1.89±0.07 •	2.09±0.06 *
Urine Pi (mmol/L)	35.22±0.98	38.12±0.73 •	36.33±0.79 *

All values are presented as mean±SD, •$p < 0.05$ vs. SO, *$p < 0.05$ vs. Orx.

was 5% ($p < 0.05$) lower after Ca^{2+} treatment (Orx+Ca) than in the Orx group.

Discussion

Increased bone turnover and the risk of osteoporotic bone fractures represent the common adverse events in andropausal men, mainly caused by an age-related decline in the serum testosterone level. Due to decreased dietary calcium intake and its diminished absorption from the small intestine in elderly (8), accompanied with an increase in PTH concentration (13), calcium supplementation is widely used for the prevention and treatment of advanced-age osteoporosis (10). In the present study, we investigated the effects of chronic Ca^{2+} treatment on the structure and function of PTG, NaPi 2a and PTH1R in the proximal kidney tubules of middle-aged male orchidectomized rats, as an animal model of the andropause. Pi reabsorption in the proximal tubules is dominantly NaPi 2a mediated, whose downregulation with PTH is realized through the extracellular-signal-regulated kinases 1/2 (ERK1/2) signaling pathway (21).

In Orx middle-aged rats, the lack of steroid hormones induced a significant increase in PTG volume, volume density of its chief cells and serum PTH. Furthermore, the ultrastructural analysis showed numerous, finger-like cell membrane invaginations in Orx animals together with well developed RER and Golgi complex, as well as a large number of mitochondria, when compared to SO rats. As suggested by Coleman and Silberman (22), these ultrastructural features appear to be reliable indicators of increased PTH synthesis. In addition, the observed reduction of serum Ca^{2+} concentration after Orx also contributes to the rise in PTH concentration (19). Furthermore, it is established that low serum Ca^{2+} concentration regulates PTH mRNA stability posttranscriptionally, through the interactions of RNA-binding protein with the PTH mRNA (23). Treatment with Ca^{2+} in our experimental conditions led to significantly decreased PTG volume, Vvcc and serum PTH concentration, in comparison with the Orx animals. However, Vvi was

significantly increased after Ca^{2+} treatment, when compared to Orx rats, which further lowers the PTG chief cells secretory potential. Ultrastructural analysis of chief cells after Ca^{2+} treatment revealed less prominent interdigitations on the chief cells' membrane, together with poorly developed RER and Golgi complex, and fewer mitochondria. Inhibitory effect of Ca^{2+} treatment on the histomorphometric and ultrastructural characteristics of PTG chief cells, together with the expected increase in Ca^{2+} serum concentration we observed, is in line with the previously shown decreased synthesis and secretion of PTH, mediated by calcium-sensing receptor (CaR) activation (24, 25).

The biochemical findings showed a significant increase in Pi urinary excretion, together with a decrease in serum Ca^{2+} and Pi concentrations after Orx, which is consistent with our previous results (17–19). The observed increase in urine Pi concentration after Orx could be a consequence of the reduced expression of NaPi 2a cotransporter in the epithelial cells of kidney proximal tubules (19). In addition, the observed increase in the immunofluorescent signal of PTH1R in Orx animals' epithelial cells of the kidney proximal tubules could also point to reduced Pi uptake from primary urine. Namely, since PTH has a stimulatory effect on PTH1R mRNA stability (26), an increased presence of PTH1R could provide the inhibitory effect of PTH on abundance of NaPi 2a (27, 28). After Ca^{2+} treatment, the expected increase in serum Ca^{2+} occurred, together with a rise in serum Pi concentration, the latter implying enhancement of Pi reabsorption rate from the urine. Treatment with Ca^{2+} slightly increased NaPi 2a cotransporter gene expression and its immunofluorescent signal on the BBM of epithelial cells of the kidney proximal tubules, when compared to Orx animals. However, the presence of PTH1R was reduced after Ca^{2+} administration, which could be in accordance with the reduction in PTH serum concentration (26). Additionally, the increment of serum Ca^{2+} concentration could activate CaR in proximal tubule cells and specifically attenuate PTH-suppressible Pi absorption in the epithelial cells of kidney proximal tubules (29).

Our study showed that Ca^{2+} administration reduced the PTH serum level and the presence of PTH1R, while the increased abundance of NaPi 2a cotransporter induced an enhancement of Pi urine reabsorption in an animal model of the andropause. These findings suggest that the use of Ca^{2+} in the prevention and treatment of andropausal symptoms implicates some mineral metabolism beneficial effects, but further studies are needed for the clarification of the exact mechanisms of its action.

Conflict of interest statement

The authors stated that there are no conflicts of interest regarding the publication of this article.

References

1. Proceedings of the Endocrine Society Andropause Consensus Conference 2000–2001. Monograph.

2. Vance ML. Andropause. Growth Horm IGF Res 2003; 13: S90–2.

3. Morales A. Andropause (or symptomatic late-onset hypogonadism): facts, fiction and controversies. The Aging Male 2004; 7: 297–303.

4. Bilezikian JP, Morishima A, Bell J, Grumbach MM. Increased bone mass as a result of estrogen therapy in a man with aromatase deficiency. New Engl J Med 1998; 339: 599–603.

5. Vanderschueren D, Vandenput L, Boonen S, Lindberg MK, Bouillon R, Ohlsson C. Androgens and bone. Endocr Rev 2004; 25: 389–425.

6. Matsumoto C, Inada M, Toda K, Miyaura K. Estrogen and androgen play distinct roles in bone turnover in male mice before and after reaching sexual maturity. Bone 2006; 38: 220–6.

7. Moutsatsou P. The spectrum of phytoestrogens in nature: our knowledge is expanding. Hormones 2007; 6: 173–93.

8. Nuti R. Calcium supplementation and risk of cardiovascular disease. Clinical Cases in Mineral and Bone Metabolism 2012; 9: 133–4.

9. Gennari C. Calcium and vitamin D nutrition and bone disease of the elderly. Public Health Nutrition 2001; 4: 547–59.

10. Tang BMP, Eslick GD, Nowson C, Smith C, Bensoussan A. Use of calcium or calcium in combination with vitamin D supplementation to prevent fractures and bone loss in people aged 50 years and older: a meta-analysis. The Lancet 2007; 370: 657–66.

11. Bolland MJ, Avenell A, Baron JA, Grey A, MacLennan GS, Gamble GD, et al. Effect of calcium supplements on risk of myocardial infarction and cardiovascular events: meta-analysis. BMJ 2010; 341: C3691.

12. Yano S, Brown EM. The calcium sensing receptor. In: Naveh-Many T, editor. Molecular biology of the parathyroid. Kluwer Academic, Plenium Publishers, New York, New York, USA, 2002.

13. Halloran B, Uden P, Duh QY, Kikuchi S, Wieder T, Cao J, et al. Parathyroid gland volume increases with postmaturational aging in the rat. American Journal of Physiology Endocrinology and Metabolism 2002; 282: 557–63.

14. Bikle D. Hormonal regulation of bone mineral homeostasis. Touch Briefings 2008; 70–4.

15. Biber J, Hernando N, Forster I, Murer H. Regulation of phosphate transport in proximal tubules. Pflügers Archiv European Journal of Physiology 2009; 458: 39–52.

16. Nordin BE. Calcium and osteoporosis. Nutrition 1997; 13: 664–84.

17. Filipović B, Šošić-Jurjević B, Ajdžanović V, Trifunović S, Manojlović-Stojanoski M, Ristić N, et al. The effect of orchidectomy on thyroid C cells and bone histomorphometry in middle-aged rats. Histochem Cell Biol 2007; 128: 153–9.

18. Filipović B, Šošić-Jurjević B, Ajdžanović V, Brkić D, Manojlović-Stojanoski M, Milošević V, et al. Daidzein administration positively affects thyroid C cells and bone structure in orchidectomized middle-aged rats. Osteoporosis Int 2010; 2: 1609–16.

19. Pantelić J, Ajdžanović V, Medigović I, Mojić M, Trifunović S, Milošević V, et al. J Physiol Pharmacol 2013; 64: 361–8.

20. Gundersen HJ, Jensen EB. The efficiency of systematic sampling in stereology and its prediction. J Microscopy 1987; 147: 229–63.

21. Bacic D, Schulz N, Biber J, Kaissling B, Murer H, Wagner CA. Involvement of the MAPK-kinase pathway in the PTH-mediated regulation of the proximal tubule type IIa Na+/Pi cotransporter in mouse kidney. Pflügers Arch Eur J Physiol 2003; 446: 52–60.

22. Coleman R, Silbermann M. Ultrastructure of parathyroid glands in triamcinolone-treated mice. J Anat 1978; 126: 181–92.

23. Naveh-Many T. The play of proteins on the parathyroid hormone messenger ribonucleic acid regulates its expression. Endocrinology 2010; 151: 1398–402.

24. Babić N. Clinical phramacogenomics and concept of personalized medicine. J Med Biochem 2012; 31: 281–6.

25. Galitzer H, Lavi-Moshayoff V, Nechama M, Meir T, Silver J, Naveh-Many T. The calcium-sensing receptor regulates parathyroid hormone gene expression in transfected HEK293 cells. BMC Biology 2009; 7: 17.

26. Josifovska T, Nonoguchi H, Machida K, Tomita K. Mechanisms of down-regulation of the renal parathyroid hormone receptor in rats with chronic renal failure. Nephron Exp Nephrol 2003; 93: 141–9.

27. Kempson SA, Lötscher M, Kaissling B, Biber J, Murer H, Levi M. Parathyroid hormone action on phosphate trans-porter mRNA and protein in rat renal proximal tubules. Am J Physiol 1995; 268: 784–91.

28. Bacic D, LeHir M, Biber J, Kaissling B, Murer H, Wagner CA. The renal Na+/phosphate cotransporterNaPi-IIa is internalized via the receptor-mediated endocytic route in response to parathyroid hormone. Kidney Int 2006; 69: 495–503.

29. Ba J, Brown D, Friedman PA. Calcium-sensing receptor regulation of PTH-inhibitable proximal tubule phosphate transport. Am J Physiol Renal Physiol 2003; 285: 1233–43.